

Impedance Analysis of Gellan Gum - Poly(vinyl pyrrolidone) Membranes

S. R. MAJID,¹ R. C. SABADINI,² J. KANICKI,³
AND A. PAWLICKA^{2,3,*}

¹Centre for Ionics University of Malaya, Physics Department, University of Malaya, Kuala Lumpur, Malaysia

²IQSC-Universidade de São Paulo, São Carlos-SP, Brazil

³Department of Electrical Engineering and Computer Science, University of Michigan, Ann Arbor, MI, USA

This paper presents the impedance study of low acyl gellan gum/poly(vinyl pyrrolidone) blend as a host matrix for ion conduction. Low salt content of lithium perchlorate was added into the blend polymer host and the membranes were prepared by the means of solution casting method. The temperature-conductivity of the investigated samples follows the Vogel-Tamann-Fulcher rule. The occurrence of electrode polarization was explained by the combination of the dielectric loss, tangent loss and imaginary part of conductivity. The relaxation time for dipole orientation and ionic conductivity were calculated from tangent loss and imaginary part of modulus.

Keywords Polymer electrolyte; natural polymer; impedance

Introduction

Dielectric relaxation in solids has been a subject of intense studies in physics domain since the 18th century [1]. The development of new materials, including multicomponent ones and curiosity to understand better the charge behavior in materials became also interesting for the chemistry and electrical engineering domains [2]. The dielectric relaxation can be obtained from impedance analysis which also provides information about the physical and chemical state of studied systems [3].

The bio-materials are known ever since and principally used in construction, textile industry and in the production of small utensils as well as processed in the food and pharmaceutical industry due to their high nutrition value and nice taste [4, 5].

Concerning engineering applications, natural macromolecules are very interesting materials as ionic conducting membranes on substitution of liquid electrolytes in electrochemical devices, as batteries, solar cells, organic light emitting diodes or electrochromic devices [6]. For such purpose, different polysaccharides and their derivatives [7–9] and proteins are proposed [10, 11].

*Address correspondence to Agnieszka Pawlicka, IQSC-Universidade de São Paulo, Av. Trabalhador São-carlense, 400, 13566-590 São Carlos, São Paulo, Brazil; E-mail: agnieszka@iqsc.usp.br

Color versions of one or more of the figures in the article can be found online at www.tandfonline.com/gmcl.

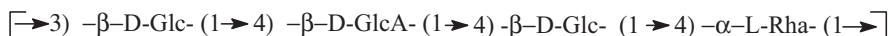
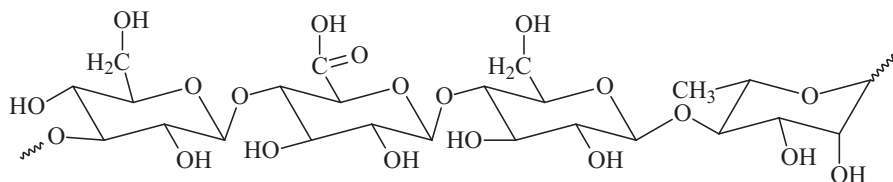


Figure 1. Chemical structure of gellan gum after deacetylation process.

Gellan gum is an anionic polysaccharide produced by the fermentation of pure culture of *Sphingomonas elodea* [12, 13]. It is a multifunctional gelling agent that can be used either alone or in combination with other products to obtain a wide variety of interesting textures, including the reversible properties under heating and cooling [14, 15]. It has been primarily studied in the field of ophthalmology for the development of new lenses with drug-delivery properties [16]. As the gum poses no danger to humans it has also been researched to be used as a stabilizer and thickener in foods, which means that can produce gel texture ranging from hard and brittle to fluid [5, 17, 18].

From the standpoint of the chemical structure, gellan gum is an heteropolysaccharide composed of repetitive units of tetrasaccharides consisting of two glucoses (Glc), one glucuronic acid (GlcA) and one rhamnose (Rha) rings (Fig. 1).

The uniqueness of gellan gum is its ability to produce solutions with low viscosity of 0.031 Pa.s (0.4% of gellan gum in ultra-pure water at 20°C and 116 s⁻¹ shear rate) [5, 18]. Thus, gellan gels can be prepared with only 0.04 to 0.05% (w/v) of this polysaccharide and after introduction of calcium, magnesium or potassium ions this concentration can be reduced [5], similarly to sodium alginate [19]. Another important property of gellan gum gels is their high thermal stability up to 120°C. Consequently, highly transparent and temperature stable membrane which can accommodate chemical substances in the form or not of ions are prepared and studied with the purpose to be applied in ophthalmology and/or more recently in electrochemical devices too [20].

Aiming to investigate the possibility of low acyl gellan gum/poly(vinyl pyrrolidone) (GGLA/PVP) blend synthesis new membranes were obtained and analyzed throughout electrical, thermal and microscopic properties. PVP was chosen due to its solubility in polar solvents including water and also good environmental stability, easy processability and moderate electrical conductivity [2].

The dielectric properties such as dielectric loss, an electrode and interfacial polarization effect of polymeric blends are very important for the device applications such as capacitors, insulators and conductors among others [2]. However, these properties can be affected by quantity of additives and/or dopants used in multicomponent system formulation [21]. Thus, the dielectric relaxation spectroscopy has been widely used to analyze the changes in such systems after plasticizer and/or salt addition. In this work, dielectric behaviors of GGLA/PVP-based membrane sample doped with salt content of 2 to 16 wt% were studied in terms of *ac* conductivity dielectric constant, dielectric loss, tangent loss and electric modulus.

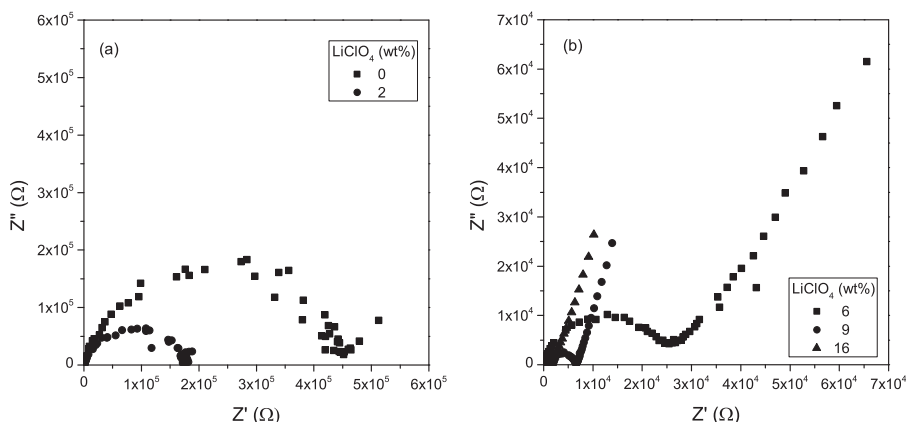


Figure 2. Nyquist diagrams of GGLA/PVP ionic conducting membranes with 0 and 2 wt% (a) and with 6, 9 and 16 wt% (b) of LiClO_4 .

Experimental

The polymer blend samples were prepared by dissolving low acyl gellan gum (GGLA; Kelco) and poly(vinyl pyrrolidone) (PVP; Aldrich) with 1:1 weight ratio in Milli-Q[®] water with controlled resistivity of 18 M Ω cm at 25 °C. To ensure complete dissolution, Milli-Q[®] water was heated at 60 °C before the addition of the polymers. Different amounts of lithium perchlorate (LiClO_4) ranging from 2 to 16 wt% were then added to the solution and stirred at room temperature for 24 hours to obtain a homogenous mixture. The final solution was poured into a plastic petri plate and dried at 40 °C for 48 hours, resulting in free standing membranes, which were stored in a desiccator to avoid air humidity and for further characterizations.

The samples were analyzed by Scanning Electron Microscopy (SEM; not showed here) performed with LEO apparatus under up to 20,000x magnification evidencing very uniform and homogeneous surface without any cracks and imperfections.

The impedance measurements were performed by sandwiching the 1.54 cm round and about 5 μm thick membranes between two mirror-polished stainless-steel 304 electrodes [11]. The measurements were performed in vacuum using a home-made Teflon[®] sample holder and, Solartron SI 1260 Impedance/Gain Phase Analyzer coupled to a computer in the frequency range of 10^7 to 0.1 Hz with amplitude of 5 mV and temperature range from 303 K to 373 K and EDG 5P oven.

Results and Discussion

The electrical impedance of the studied samples was measured as a function of temperature in order to analyze the ionic conductivity values and dielectric properties of the samples. The Nyquist plots used to obtain ionic conductivity values of the GGLA/PVP samples without and with 2 to 16% of LiClO_4 as a function of temperature are shown in Fig. 2. As can be seen in Fig. 2a, the region of semicircle at high frequencies in the complex plane corresponding to the electrolyte resistance and from which it is possible to obtain ionic conductivity values is very big and shows very high real resistance for the sample without lithium salt. The addition of LiClO_4 in the sample formulation promotes a decrease of its

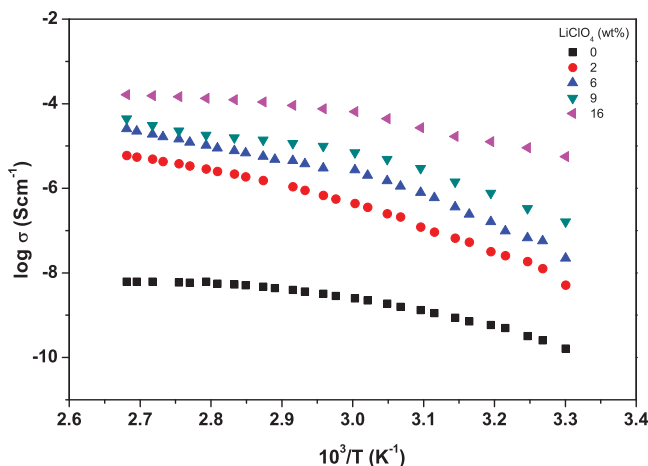


Figure 3. Plots of *dc* conductivity versus inverse of temperature of GGLA/PVP with different (0–16 wt%) salt content.

real resistance values (Figs. 2a and 2b) however the semicircle is still observed. Moreover, all the samples showed a decrease in the semicircle with the increase of temperature from 303 to 373 K. Also these results are very similar to the pectin-based samples [22].

The electrolyte bulk resistance (R_b) was obtained from the intercept of the semicircle with the Nyquist plot real axis. Then the *dc* ionic conductivity was deduced from the R_b values by employing the formula $\sigma = l/R_b A$, where l was the thickness of the electrolyte sample and A was the contact area between the electrolyte and the electrode. Fig. 3 shows the ionic conductivity values as a function of temperature for the samples with different salt contents ranging from 0 to 16 wt%. From this figure it can be observed that, in the salt free polymer blend sample, as expected the conductivity is very low, i.e., of 1.6×10^{-10} S/cm at 303 K and increases one order of magnitude to 6.2×10^{-9} S/cm with temperature until 373 K. The curved shape of the experimental data plotted in this figure indicates that the ionic conductivity is governed mostly by the Vogel-Tamann-Fulcher (VTF) than Arrhenius ionic conduction model. The VTF model suggests that the ionic conductivity is due to the segmental motion of the polymer chain in the matrix [23]. In this case, this phenomenon can be addressed to the intra- and interchain segmental motions in the blended polymer matrix, which serve as vehicle to Li^+ ionic transport [24]. The low ionic conductivity value suggests an insulating property as observed in the case of PVP-starch blend [2]. An increase of the salt content also promotes a gradual increase of the ionic conductivity to 5.6×10^{-6} S/cm at 303 K for the sample with 16 wt% of LiClO_4 . Accordingly to other polysaccharides conducting membranes this is certainly related to the increase in the number of mobile charge carriers due to the added salt [6].

Aiming to understand better the ion conduction mechanism in the studied samples the frequency dependence of *ac* electrical conductivity ($\sigma = \sigma_0 + A\omega^n$ where σ_0 is a *dc* conductivity, A – pre exponent factor and n – power law exponent [25] and/or temperature dependent constant [26]) at different temperatures for all studied samples is displayed in Fig. 4. The trend of the conductivity spectrum shows the switch over frequency (f) at which the *dc* conductivity plateau obtained is increased with increasing of temperature. The switchover from the frequency-independent to the frequency-dependent regions indicates that the starting point of the conductivity relaxation is increased and the way of ion

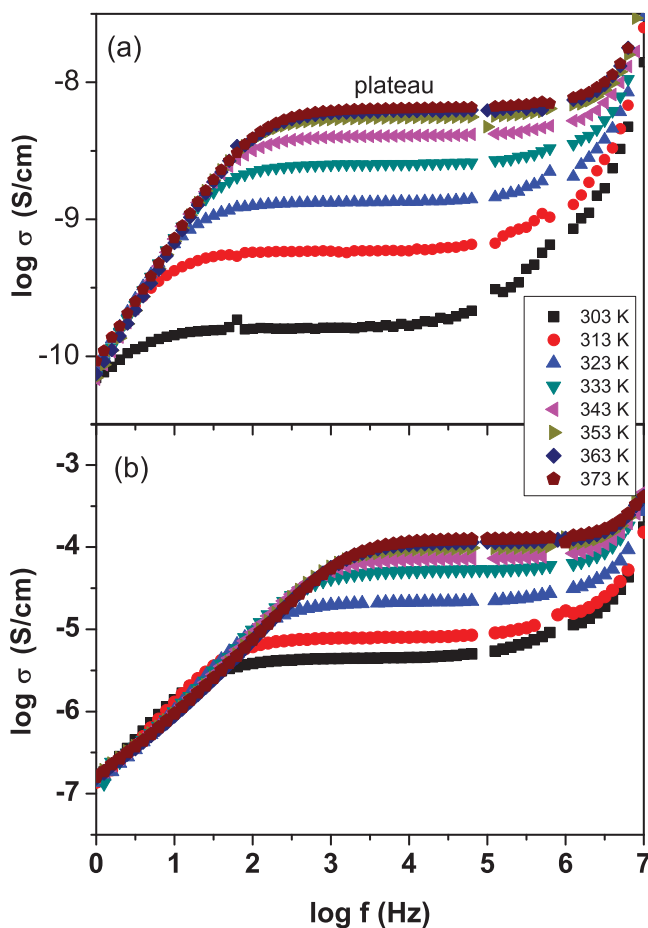


Figure 4. Frequency-dependent real part of *ac* conductivities of pure GGLA/PVP blend (a) and with 16 wt% of LiClO_4 (b).

conduction has been changing from long range translation to the short range ion motion. At low frequency region, i.e., before the *dc* conductivity plateau, the dispersion in conductivity can be ascribed to the electrode polarization which can be further justified in ϵ'' ($\epsilon'' = \frac{Z'}{\omega C_o(Z'^2 + Z''^2)}$ where Z' and Z'' are real and imaginary part of impedance, C_o is the capacitance of empty measuring cell and ω is angular frequency) and σ'' versus frequency plots [25, 27].

The variation of dielectric constant ($\epsilon' = \frac{Z''}{\omega C_o(Z'^2 + Z''^2)}$) with frequency at different temperatures for GGLA/PVP blend and its complexes is depicted in Fig. 5. The dielectric constant (ϵ') is resulted from the total polarization arising from the trapped charge as well as dipoles in the materials [28]. For strong polar polymers, dielectric constant value will increase with temperatures because of its ability to align themselves within the applied field direction after thermal energy absorption. In the present study, the data presented in Fig. 5a indicates the strong polar nature of GGLA/PVP blend sample. The dielectric constant of pure GGLA/PVP blend is observed to increase with increase of temperature. At low frequency region, the initial value of the dielectric permittivity is high for polar

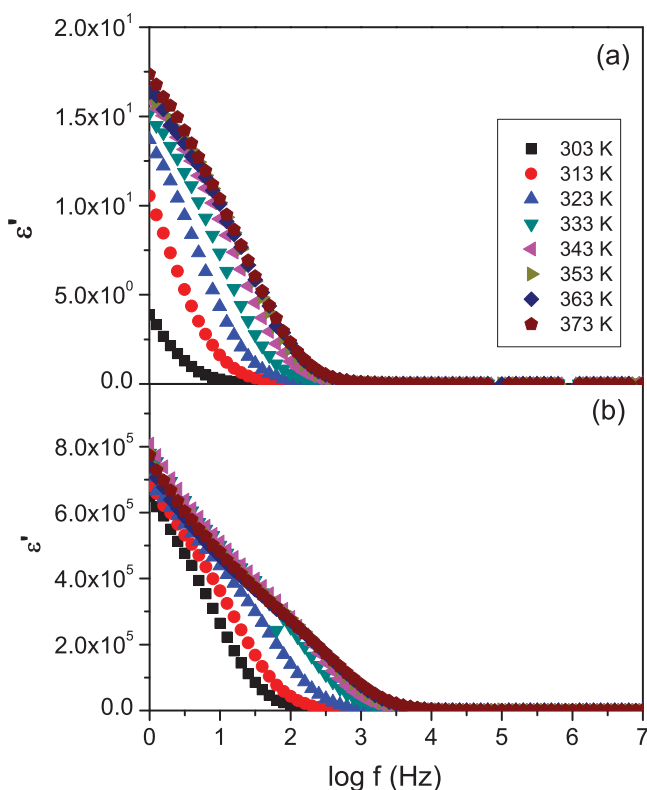


Figure 5. Frequency-dependent dielectric constant for pure GGLA/PVP blend (a) and with 16 wt% of LiClO_4 (b).

materials, but as the frequency of the field is increased the value starts to drop. According to the literature the drop is an indication of the scattered dipoles that are not being able to follow the field variation at high frequencies [2] and also may be due to the polarization effects [28, 29]. Meanwhile, in the blend complexes, when LiClO_4 content is increased, the trapped charge carriers in polymer blend is increased hence the dielectric constant value is increased as showed in Fig. 5b for the sample with 16 wt% of LiClO_4 . At low frequencies the increase in dielectric constant with increase of the salt content is in good agreement with dielectric behaviour of PMMA- LiCF_3SO_3 polymer electrolyte [30]. Hence, it is found that the temperature largely influences the dielectric constant of the samples [31].

The spectra of the imaginary part of permittivity (ϵ'') and imaginary part of ac conductivity ($\log \sigma(\omega)$, where $\sigma(\omega) = \sigma(0) + A\omega^n$; $\sigma(0)$ is dc conductivity subtracted from experimental $\sigma(\omega)$, A is pre-exponent factor and n is power law exponent [25, 27]) as a function of frequency are shown in Figs. 6 and 7 at different temperatures, respectively. In all polymer blend-salt complexes, at low frequency region the dielectric loss values tends to become very large ($\sim 10^5$) as a results of free charge motion within the material [2]. As in other studies these values are most probably due to the free charges present at the contact surface between the polymeric electrolyte sample and the electrodes [30]. In all studied samples here, ϵ'' increases with decreasing frequency (Fig. 6) which corresponds to electrode polarization phenomena [28]. At low frequency region, the spectra shows distinguishable peak that corresponds to the relaxation peak of electrode polarization and

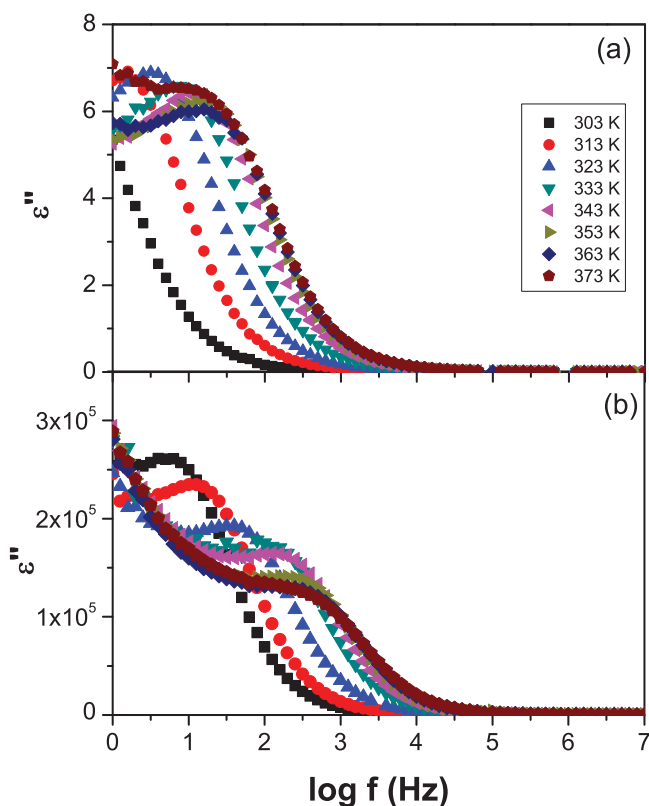


Figure 6. Frequency-dependent dielectric loss of (a) pure GGLA/PVP blend and (b) containing 16 wt% of LiClO_4 .

the peak position is influenced by the temperature (Fig. 6a). The higher salt content the higher frequency peaks were observed indicating that the addition of LiClO_4 leads to a significant change in the electrical response of GGLA/PVP blend sample (Fig. 6b). Further, the electrode polarization relaxation peak in the investigated samples were analyzed from the temperature dependence of the imaginary part of log of conductivity as shown in Fig. 7.

Afore mentioned, the relaxation in the low frequency region occurs as a result of an accumulation of ions at the electrode/sample interface. The imaginary part of conductivity was used to demonstrate further the relaxation phenomena at low frequency region. The frequency peak of $\log \sigma''$ - frequency plot (Fig. 7) is almost the same with the peak frequency of ϵ'' - frequency (Fig. 6) implying that the relaxation peak at low frequency is attributed to electrode polarization.

At this point it should be stated that the Differential Scanning Calorimetry (DSC; not shown here) analysis of the samples with 2, 6, 9 and 16% of lithium salt revealed the glass transition temperature (T_g) values of about 263 K, thus below the impedance measurements temperature interval. Consequently, there is no influence of T_g on relaxation. Aiming at gaining further information on the dielectric behavior of polymer blend and its complexes, $\tan \delta$ ($\tan \delta = \frac{\epsilon''}{\epsilon'} = \frac{M''}{M'}$) [32] was plotted as a function of frequency at various temperatures, as shown in Fig. 8. The largest influence of electrode polarization and structural relaxations can be studied in frequency region from 0.1 Hz to 1 MHz. Since the contribution of

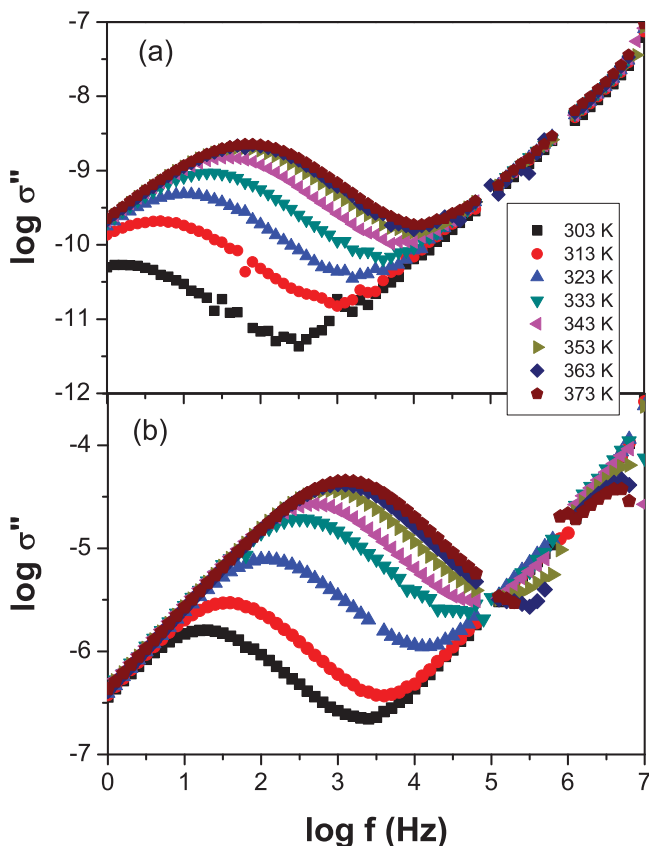


Figure 7. Frequency-imaginary part of *ac* conductivity for pure GGLA/PVP blend (a) and containing 16 wt% of LiClO₄ (b).

electrode polarization can be elucidated from ε'' -frequency and $\log \sigma''$ -frequency plots, peak in $\tan \delta$ spectra can suggest on different contribution to ionic conduction processes, i.e., most probably due to dipole orientation in the macromolecules [28–31]. The position shifts of $\tan \delta$ peak imply the variations of the relaxation time for ionic conduction process as a function of temperature. Since the $\tan \delta$ is deeply influenced by the presence of ionic charges, the contribution of dipole orientation in the macromolecules to the conductivity of the samples can be manifested from the relaxation time ($\tau = \omega^{-1}$), which can be calculated from the frequency peak in $\tan \delta$ -frequency (ω) spectra. As can be noted in Fig. 9, the τ values of the polymer-salt complexes indicate that the higher salt concentration the faster charge movement, which could be governed by the salt concentration and inter- and intramolecular bonding in the samples. The linear decrease in the relaxation time with an increase of temperature suggests the miscibility of the polymer and salt due to the hydrogen bond formation as in the case of the PVP-starch [31]. Moreover, the decrease of the relaxation time with increase of the salt concentration in the sample and consequently increase of the ionic conductivity was already observed in polymer electrolytes based on poly(ε -caprolactone) [33].

Depicted in Fig. 10 is the dielectric data in the electric modulus presentation, which is useful to minimize the variations in large values of the dielectric constant and conductivity at

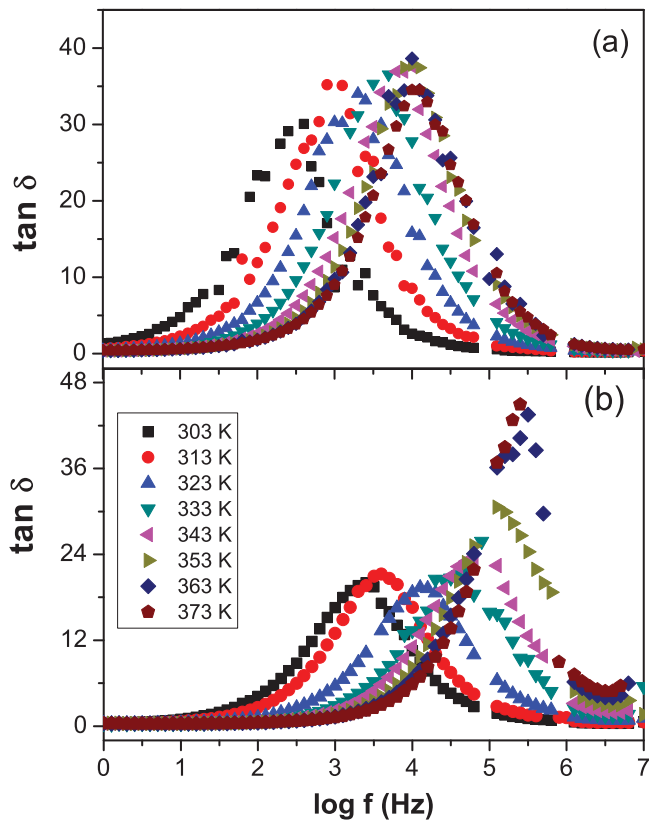


Figure 8. Frequency-dependent tangent loss of (a) pure GGLA/PVP blend and (b) containing 16 wt% of LiClO_4 .

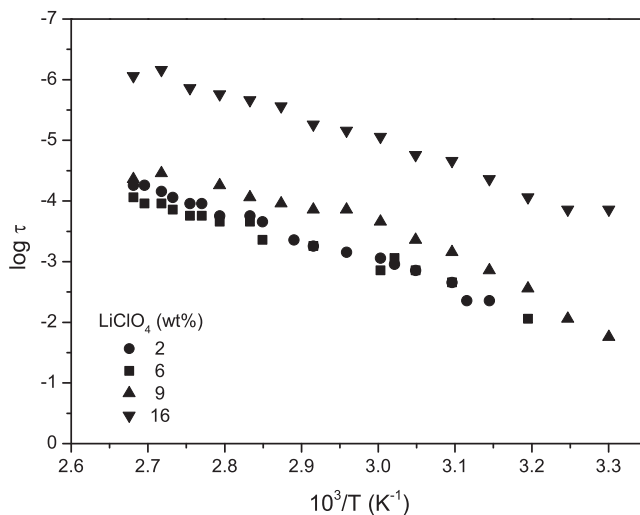


Figure 9. Relaxation time of electrode polarization as a function of temperature for the samples of GGLA/PVP with 2, 6, 9 and 16 wt% of LiClO_4 .

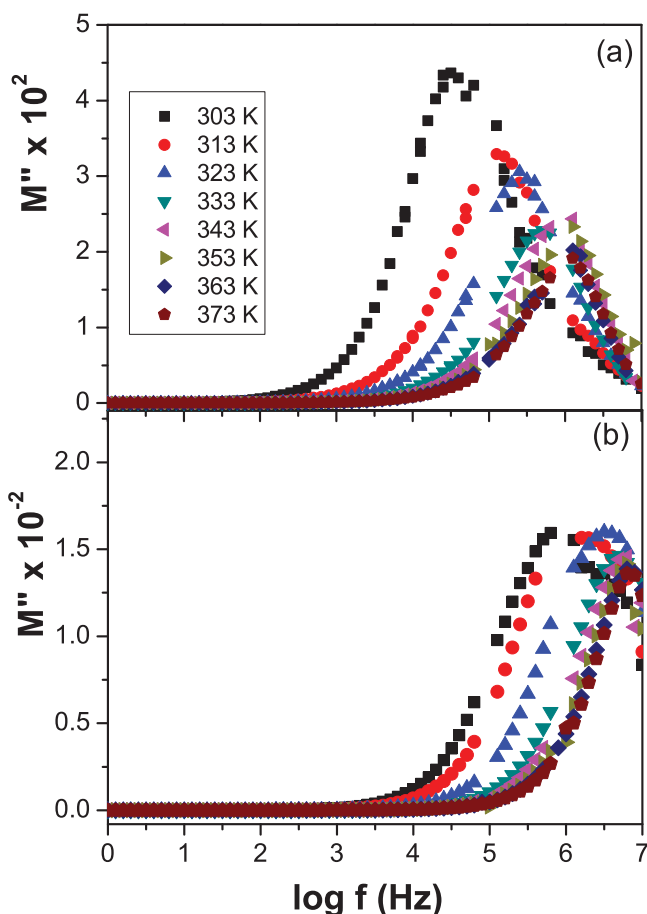


Figure 10. Frequency-dependent imaginary part of modulus for (a) pure GGLA/PVP blend and (b) containing 16 wt% of LiClO_4 .

low frequencies. The problems with electrode nature and contact, the electrode polarization as well as space-charge injection phenomena and/or absorbed impurity conduction effects, which can appear in relaxation data, can be neglected [34, 35]. Thus the electric modulus was obtained through [27],

$$M' = \frac{\varepsilon'}{(\varepsilon'^2 + \varepsilon''^2)}$$

$$M'' = \frac{\varepsilon''}{(\varepsilon'^2 + \varepsilon''^2)}$$

As seen from the Fig. 10, the low values of M'' in the low frequency region show the removal of the electrode polarization to the electric modulus. Broad and asymmetric peak at high frequencies region are observed in all samples which is due to consequence of relaxation time distributions [33, 34]. The frequency region below the maximum peak determines the range in which charge carriers are mobile on long distances. The peak frequency in the frequency dependent M'' plot shifts to higher frequencies as the temperature

increases implying that the system stabilizes in a short time for an external force at elevated temperatures.

From the electrical modulus formalism, the temperature and frequency dependencies of dielectric properties of the GGLA/PVP-LiClO₄ samples can be explained as follows: when the temperature is raised, the GGLA/PVP matrix become softer, due to the melting of the sample (DMTA data not shown here). At the same time the salt dissociate at high rate and probably coordinate with oxygen atom [36]. Thus, the interaction between GGLA/PVP blend matrix and LiClO₄ enhance, and consequently the dielectric constant increases.

Conclusions

Low acyl gellan gum/poly(vinyl pyrrolidone) blend without and with LiClO₄ were obtained and characterized by impedance spectroscopy as a host matrix for ion conduction. The ionic conductivity of 1.6×10^{-10} S/cm revealed insulator properties of the samples without salt. The addition of the LiClO₄ to the sample formulation promoted an increase of the ionic conductivity values to 5.6×10^{-6} S/cm at 303 K and 1.6×10^{-4} S/cm at 373 K for the sample with 16 wt% of LiClO₄. The ionic conductivity as a function of temperature of all investigated samples obeyed VTF ionic conduction model. Moreover, the occurrence of electrode polarization was interpreted from the dielectric loss, tangent loss and imaginary part of conductivity. The relaxation times as a function of frequency for dipole orientation and ionic conductivity were calculated from tangent loss and imaginary part of modulus. The highest ionic conductivity value was observed for the lowest relaxation time. Additionally, it was stated that the linear decrease in the relaxation time of dipole orientation suggest the miscibility of the polymer and salt due to the hydrogen bond formation and corroborate to the dielectric constant discussion.

Acknowledgments

The financial support of the Brazilian agencies Capes, CNPq and FAPESP are gratefully acknowledged. The author is also grateful to Dr. Ana Paula Garcia Ferreira from IQSC for DSC analysis.

References

- [1] Jonscher, A. K. (1999). *Journal of Physics D-Applied Physics*, 32, R57.
- [2] Reddy, C. V. S., Han, X., Zhu, Q. Y., Mai, L. Q., & Chen, W. (2006). *Microelectronic Engineering*, 83, 281.
- [3] Macdonald, J. R. (1992). *Annals of Biomedical Engineering*, 20, 289.
- [4] Pawlicka, A., Grote, J., Kajzar, F., Rau, I., & Silva, M. M. (2012). *Nonlin. Optics Quant. Optics*, 45, 113.
- [5] Giavasis, I., Harvey, L. M., & McNeil, B. (2000). *Critical Reviews in Biotechnology*, 20, 177.
- [6] Pawlicka, A., & Donoso, J. P. (2010). Polymer electrolytes based on natural polymers, in: C. A. C. Sequeira and D. M. F. Santos (Eds.) *Polymer Electrolytes: Properties and Applications*, Woodhead Publishing Limited, Cambridge, p. 95.
- [7] Pawlicka, A., Sabadini, A. C., Raphael, E., & Dragunski, D. C. (2008). *Mol. Cryst. Liq. Cryst.*, 485, 804.
- [8] Pawlicka, A., Danczuk, M., Wieczorek, W., & Zygadlo-Monikowska, E. (2008). *J. Phys. Chem. A*, 112, 8888.
- [9] Fuentes, S., Retuert, P. J., & Gonzalez, G. (2007). *Electrochim. Acta*, 53, 1417.
- [10] Vieira, D. F., Avellaneda, C. O., & Pawlicka, A. (2007). *Electrochim. Acta*, 53, 1404.

- [11] Vieira, D. F., & Pawlicka, A. (2010). *Electrochim. Acta*, 55, 1489.
- [12] Ramaiah, S., Kumar, T. M. P., & Ravi, V. (2007). *J. Macromol. Sci. A*, 44, 229.
- [13] Jansson, P. E., Lindberg, B., & Sandford, P. A. (1983). *Carbohydrate Res.*, 124, 135.
- [14] Ramaiah, S., Kumar, T. M. P., & Shah, J. (2007). *Latest Reviews*, 5.
- [15] Miyoshi, E., Takaya, T., & Nishinari, K. (1996). *Carbohydrate Polym.*, 30, 109.
- [16] Paulsson, M., & Edsman, K. (2002). *J. Coll. Interface Sci.*, 248, 194.
- [17] Milas, M., Shi, X., & Rinaudo, M. (1990). *Biopolymers*, 30, 451.
- [18] Shah, J. (2007). *Gellan Gum and Its Applications – A Review*.
- [19] Moritaka, H., Nishinari, K., Taki, M., & Fukuba, H. (1995). *J. Agricult. Food Chem.*, 43, 1685.
- [20] Noor, I. S. M., Majid, S. R., Arof, A. K., Djurado, D., & Pawlicka, A. (2012). *Solid State Ionics*, 225, 649.
- [21] Rao, V., Ashokan, P. V., & Amar, J. V. (2002). *J. Appl. Polym. Sci.*, 86, 1702.
- [22] Andrade, J. R., Raphael, E., & Pawlicka, A. (2009). *Electrochim. Acta*, 54, 6479.
- [23] Cha, E. H., Macfarlane, D. R., Forsyth, M., & Lee, C. W. (2004). *Electrochim. Acta*, 50, 335.
- [24] Reddy, M. J., Sreekanth, T., & Rao, U. V. S. (1999). *Solid State Ionics*, 126, 55.
- [25] Kumar, M., Tiwari, T., & Srivastava, N. (2012). *Carbohydrate Polym.*, 88, 54.
- [26] Jonscher, A. K. (1977). *Nature*, 267, 673.
- [27] Mishra, R., Baskaran, N., Ramakrishnan, P. A., & Rao, K. J. (1998). *Solid State Ionics*, 112, 261.
- [28] North, A. M. (1972). *Chemical Society Reviews*, 1, 49.
- [29] MacDonald, J. R. (1987). *Impedance Spectroscopy: Emphasizing Solid Materials and Systems*, John Wiley & Sons, New York.
- [30] Ramesh, S., & Wong, K. C. (2009). *Ionics*, 15, 249.
- [31] El-Houssiny, A. S., Ward, A. A. M., Mansour, S. H., & Abd-El-Messieh, S. L. (2012). *J. Appl. Polym. Sci.*, 124, 3879.
- [32] Majid, S. R., & Arof, A. K. (2007). *Physica B*, 390, 209.
- [33] Woo, H. J., Majid, S. R., & Arof, A. K. (2012). *Mat. Chem. Phys.*, 134, 755.
- [34] Yu, S. Z., Hing, P., & Hu, X. (2000). *J. Appl. Phys.*, 88, 398.
- [35] Ramesh, S., & Arof, A. K. (2001). *Mater. Sci. Eng. B*, 85, 11.
- [36] Wright, P. V. (1975). *British Polym. J.*, 7, 319.